Jour. Geol. Soc. India (2022) 98:893-902
https://doi.org/10.1007/s12594-022-2092-0

ORIGINAL ARTICLE

Raman-XPS Spectroscopy, REE Chemistry, and Morphological Studies of Detrital Zircon and Monazite – Implications for Metamict State and Provenance

R. G. Rejith[a,b], M. Sundararajan[a,b*], A. Peer Mohamed[a], M. Satyanarayanan[c]

[a]Materials Science and Technology Division, CSIR-National Institute for Interdisciplinary Science and Technology (CSIR-NIIST), Thiruvananthapuram - 695 019, India.

[b]Academy of Scientific and Innovative Research (AcSIR), Ghaziabad - 201002, India

[c]Geochemistry Division, CSIR-National Geophysical Research Institute, Uppal Road, Hyderabad - 500 007, India

**E-mail: rajanmsundar77@yahoo.com*

Received: 24 July 2020 / Revised form Accepted: 31 July 2021

ABSTRACT

A combination of advanced characterisation techniques was applied to study the structure, chemistry, and surface morphological features of detrital zircon and monazite grains from the coasts of Varkala and Kovalam situated in the south-west part of India, showing implications to their metamict state, Rare Earth Element (REE) chemistry, and provenance. Raman, X-ray photoelectron spectroscopy (XPS), and Ultraviolet-Visible-near-IR (UV-Vis-NIR) spectroscopic techniques were used to detect the disorder in crystal structure due to self irradiation damage. The rare earth, radioactive, and trace elements present in these minerals were identified using high resolution inductively coupled mass spectrometer (HR-ICP-MS). These studies are also complimented by scanning electron microscope (SEM) analysis for understanding the morphological features. The present study depicts a low degree of metamictization in natural detrital zircon and monazite grains with information regarding their REE chemsitry and the surface morphological changes that occurred due to mechanical impacts caused during transportation and deposition. These vivid datasets of information facilitate the mining industry and scientific community for determining their grades.

INTRODUCTION

The Indian coast is endowed with a good quantity of strategic minerals such as ilmenite, zircon, rutile, monazite, sillimanite, garnet, etc. (Gayathri et al., 2017). The major placer deposits in India are Ratnagiri deposits (Maharashtra), Chavara (Kerala), Manavalakurichi (Tamil Nadu), Bhimunipatnam (Andhra Pradesh), and Chatrapur (Orissa) (Ali et al., 2001). Apart from these important placer deposits, many researchers have carried out detailed studies on other placer deposits namely Thiruchendur-Ovari coast in Tamil Nadu (Sundararajan, 2018), Cuddalore coast in Tamil Nadu (Viveganandan et al., 2013), Ullal and Suratkal in Karnataka (Sundararajan et al., 2009), Kanyakumari in Tamil Nadu (Sajimol et al., 2017), etc. The studies include textural characterisation and depositional environment of beach sediments (Gayathri et al., 2021; Sathasivam et al., 2015), heavy mineral analysis (Angusamy et al., 2005), mineral recovery (Rejith and Sundararajan, 2018), remote sensing exploration of beach minerals (Chandrasekar et al., 2011; Rajan Girija and Mayappan, 2019; Rejith et al., 2020a, 2020b) and geochemical characterisation (Rejith et al., 2021; Renjith et al., 2020; Sundararajan et al., 2010; Tirumalesh et al., 2020).

The beach minerals are referred to as "strategic" because of their high value in India's economy obtained by their critical applications in a wide range of areas (Nageswara Rao et al., 2001; Raju et al., 2005). These minerals act as the source for many industrial products such as rare earths, zirconium, titania, etc. The ilmenite, rutile, and leucoxene are used for manufacturing titania products such as titania pulp, titania metal, nano titania, etc. (Sundararajan et al., 2009). Synthetic mullite for refractory applications is produced from sillimanite sand, and garnet is used as an abrasive material for glass polishing (Banerjee, 1998). High purity zirconia and zircon brick are produced from zircon (Naher and Haseeb, 2006; Yamagata et al., 2008). Monazite act as the primary source for rare earth elements (Rabie, 2007; Samsonov et al., 2015). The rare earth elements include the fifteen elements in the lanthanide series (La to Lu), Sc, and Y (Balaram, 2019). The processing behaviour of beach minerals during beneficiation is very important, and that can only be determined using chemical characterisation techniques(Mitchell and Yusof, 1993). The processing behaviour of ilmenite depends on Fe_2O_3 content. Highly magnetic and conducting ilmenite contains an average of 48% Fe_2O_3, whereas, non-magnetic and non-conductive ilmenite contains only an average of 34% Fe_2O_3. In the case of zircon also, high Fe_2O_3 makes the zircon magnetic due to the inclusions of magnetite. The lower TiO_2 content makes the rutile non-conducting. All these factors significantly affect the selection of appropriate magnetic and conducting separating units for the beneficiation of these minerals. Different types of beneficiation processes were adopted for beach sand minerals based on their mineralogical and chemical composition (Kumari et al., 2015). The type and composition are the main two factors affecting the selection of treatment processes for beneficiation of rare earth oxide minerals where these two factors can only be confirmed using advanced characterisation studies (Ferron et al., 1991). Apart from recovery of minerals, chemical beneficiation of minerals like the separation of rare earth elements, Th and U from monazite, can only be carried out after determining their geochemistry(Moustafa and Abdelfattah, 2010).

The monazite grains from Chavara and Manavalakurichi deposits were analysed for their chemical composition, surface morphology, and crystal structure using ED-XRF, ICP-MS, XRD, and SEM-EDS techniques(Anitha et al., 2020; Rajendran et al., 2008). The trace elements and REEs present in zircon concentrate of beach sands from Chavara and Manavalakurichi deposits were also analysed using neutron activation analysis (Murali et al., 1983). The XRD and surface morphological analysis was carried out for zircon sand from Konark-Ramachandi coast, Orissa (Routray and Rao, 2011). The REE and trace elements present in the zircon grains of the southern coast of Tamil Nadu were determined using ICPMS (Angusamy et al., 2004). The chemical composition of monazite grains recovered from Chhatrapur in Orissa was studied using PIXE and EDXRF method (Mohanty et al., 2003). REE geochemistry of monazite from Bhimunipatnam- Konada coast in Andhra Pradesh was studied using EPMA analysis (Bangaku Naidu et al., 2016). XPS provides information regarding the chemical changes that occurred on the mineral surfaces. In the case of zircon, the formation of Zr oxide or hydroxide on mineral surfaces analysed using XPS suggests their weathering rate (Balan. et al., 2001). XPS provides information regarding the sorption of uranium (VI) species on zircon surfaces (Lomenech et al., 2003). XPS and Raman spectroscopy helps to analyse the metamictization that occurs in the zircon structure. The electronic states of O1*s* and Si2*p* states help to study the electronic structure of radiation-damaged zircon grains (Shchapova et al., 2010). The broad Raman bands between 900 and 1000 cm^{-1} indicate metamictization in detrital zircon (Zhang et al., 2000). The beneficiation of minerals, especially zircon and monazite, truly depends on the physical and chemical properties of these minerals. Advanced characterisation techniques can be used for analysing the physical and chemical properties such as the crystal structure, surface chemistry, chemical composition, and surface morphology which facilitates the grade and potential applications of these minerals.

In the present work, the crystal structure, geochemistry, and surface morphology of detrital zircon and monazite grains of Varkala and Kovalam coasts in Kerala, south-west India, have been analyzed and studied using advanced characterisation techniques such as Raman spectroscopy, XPS, UV-Vis-NIR spectroscopy, ICPMS, and SEM-EDS. The Raman spectroscopy, XPS, UV-Vis-NIR spectroscopy, and SEM-EDS were carried out at CSIR-National Institute for Interdisciplinary Science and Technology (CSIR-NIIST), Thiruvananthapuram, Kerala, India. The ICPMS was carried out at CSIR-National Geophysical Research Institute, Hyderabad, India

STUDY AREA AND PROVENANCE

The Varkala and Kovalam coasts are situated in the Thiruvananthapuram district of Kerala, located in the south-west part of India and bordered by the Lakshadweep Sea on its west (Figure 1). Geographically, the Varkala and Kovalam are located at latitudes and longitudes of 8°44’58.19"N, 76°41’41.23"E and 8°23’9.06"N, 76°58’42.23"E. The study area is situated between two major placer deposits in India, such as Chavara in Kerala and Manavalakurichi in Tamil Nadu. The beaches constitute medium to fine-sized sand with good heavy mineral content. The Varkala and Kovalam coastal stretches are endowed with a high concentration of ilmenite followed by monazite, sillimanite, rutile, zircon, garnet, and leucoxene. Minor presence of kyanite, hornblende, and sphene was also observed in these regions (Rejith et al., 2020a). The Varkala shows maximum heavy mineral content (THM%) of 52.33% with an ilmenite content of 30.985%. In the case of Kovalam, it is 80.04% with an ilmenite content of 52.86%. The maximum monazite content of heavy mineral sands of Varkala and Kovalam was estimated to about 17.44% and 18.05%.

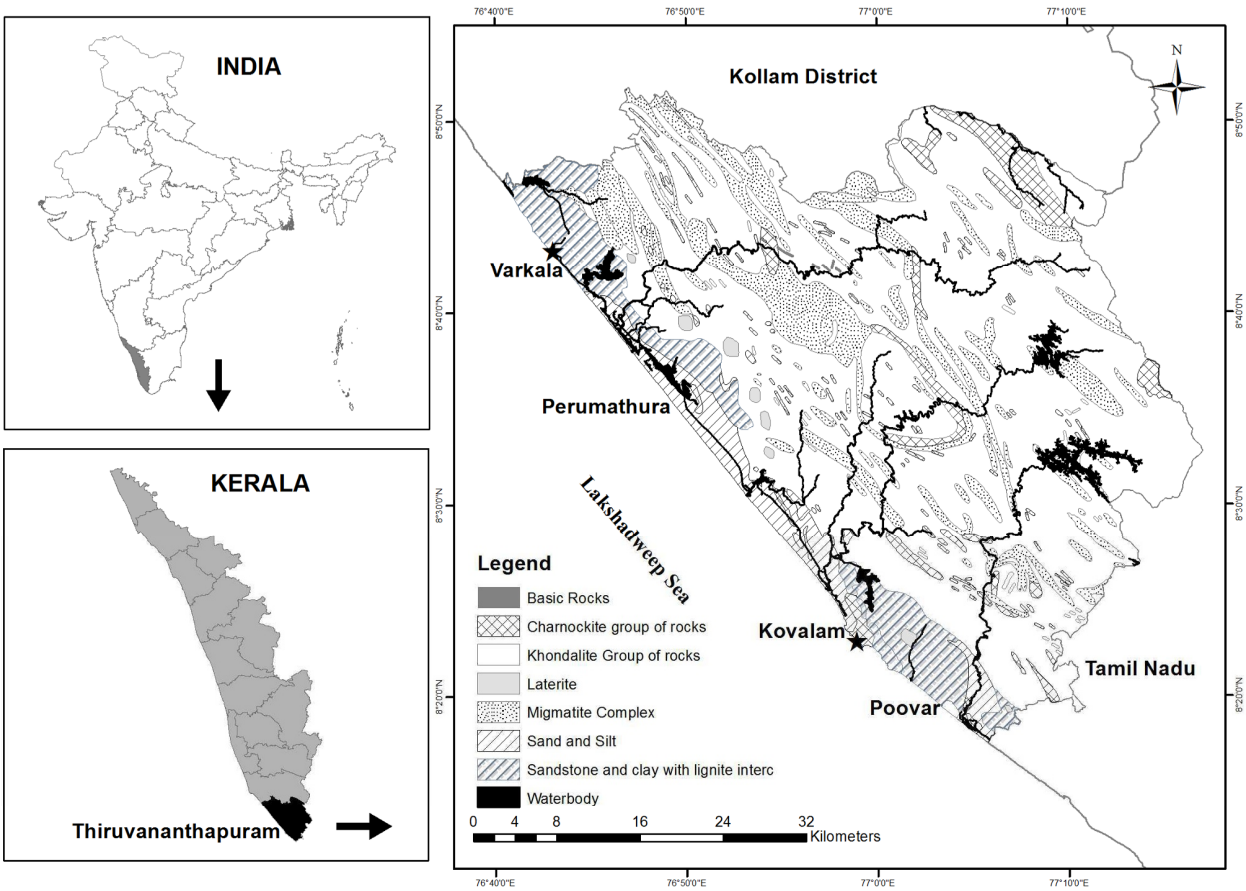

Fig.1. Study area map.

The maximum content of zircon is reported to about 0.90% and 0.17%. The minerals weathered from the host rocks (provenance) are transported by west-flowing rivers originated from the Western Ghats, and are deposited along the beaches by the actions of waves and long currents. Geologically the Thiruvananthapuram district is mainly occupied by Tertiary and Quaternary sediments on the west side along the coastal tracts and Archean crystalline rocks on the east side. The Archean crystalline rocks comprise khondalites, charnockites, and migmatite groups. The khondalites, charnockites, and the outcrops of pegmatites and quartz veins are the primary sources of these minerals. Apart from these, the Tertiary sediments and weathered laterites also play a significant role in the presence of these heavy minerals along the coast (Krishnan et al., 2001).

MATERIALS AND METHODS

Raman spectra for zircon and monazite were measured using a confocal Raman microscope (WI-Tec, Inc., Germany, alpha 300R). The XPS spectrum of zircon was taken using Multilab 2000 (Thermofisher Scientific, U.K.). The UV-Vis-NIR spectra were measured using Shimadzu UV–VIS- NIR spectrophotometer (UV-3600). The powdered bulk mineral samples were digested using HF: HNO_3 acid mixture (Satyanarayanan et al., 2018), and the content of REE, radioactive elements, and the trace elements were measured using HR-ICP-MS of make Nu Instruments Attom^R, UK at CSIR-National Geophysical Research Institute, Hyderabad, India. The SEM images were taken using JEOL make model JSM5600 LV. The chemical composition of minerals were measured using EDS instrument Silicon Drift Detector"X-MaxN attached to the SEM of Carl Zeiss make EVO18 model. The Raman spectroscopy, XPS, UV-Vis-NIR spectroscopy, and SEM-EDS were carried out at CSIR-National Institute for Interdisciplinary Science and Technology (CSIR-NIIST), Thiruvananthapuram, Kerala, India.

RESULTS AND DISCUSSION

Zircon - $ZrSiO_4$

Zircon having a tetragonal structure ($I4_1/amd$ and $Z = 4$) formed by a chain of edge-sharing and alternating SiO_4 tetrahedra (Hazen and Finger, 1979). Theoretically 12 Raman active normal modes represented as $2A_{1g} + 4B_{1g} + B_{2g} + 5E_g$ in which the internal modes are $2A_{1g} + 2B_{1g} + B_{2g} + 2E_g$ and external modes are $2B_{1g}$(translatory) + $2E_g$(translatory) + E_g(rotatory) (Dawson et al., 1971; Zhang et al., 2000). The internal modes, along with their assignments and the external modes for zircon, are listed in Table 1 (Hoskin and Rodgers, 1996; Syme et al., 1977). The Raman spectra of zircon from Varkala and Kovalam are shown in Fig.2(a). The α-decay radiations from radionuclides and their daughter products bring crystal disorders to natural zircon (Lumpkin, 2001; Weber et al., 1997). This causes the $v_3(SiO_4)$ frequency mode between 850 and 1100 cm^{-1}, to become broader and weaker (Balan. et al., 2001; Nasdala et al., 1995; Zhang et al., 2000). High radiation damage may cause loss in the periodic crystal structure of zircon and this state is termed as the metamictization of zircon (Holland and Gottfried, 1955). Metamict is defined as a state of a periodic or amorphous (Ewing, 1994). The Varkala and

Table 1. Raman frequencies (cm^{-1}) of Zircon

Symmetry	Assignment	Raman peaks (cm^{-1})
Internal modes	Si–O μ_3 stretching	1008
B_{1g}		
A_{1g}	Si–O μ_1 stretching	978
A_{1g}	Si–O μ_2 bending	439
B_{2g}	Si–O μ_2 bending	270
External modes	207, 225, 357, 395	

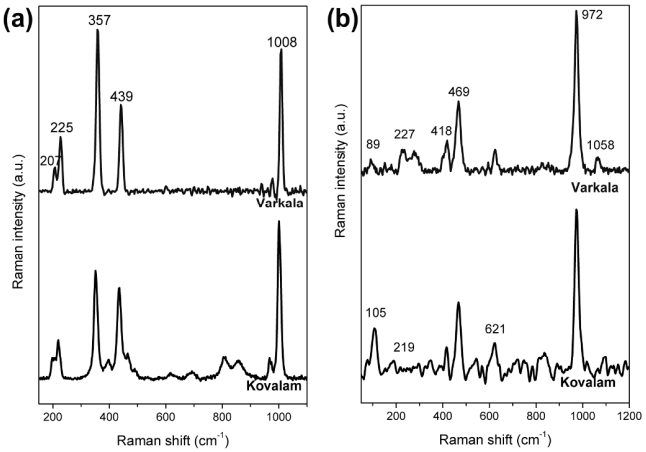

Fig. 2. Raman spectra **(a)** zircon; **(b)** monazite.

Kovalam zircon grains show a clear, well-defined peak at 1008 cm^{-1} corresponds to μ_3 (SiO_4) stretching (Dawson et al., 1971). The well-resolved and sharp peaks indicate less metamictization and a well-crystallized structure for zircon samples. The XPS peaks of the zircon are shown in Figure 3 (a-d). The Zr 3d photo-peak decomposed into $3d_{5/2}$ at 182.95 eV and $3d_{3/2}$ at 185.52 eV. The Si 2p spectra were also fitted with two Gaussian components of $Si_1$2p and $Si_2$2p at 101.10 eV and 102.27 eV (Balan. et al., 2001). The O1S represents a superposition of oxygen atoms such as O_1 and O_2 at 530.96 eV and 531.36eV. The energy of $O_1$1s corresponds to regular atoms of the three-coordinated oxygen in $ZrSiO_4$, and that of $O_2$1s corresponds to defect oxygen atoms assigned to defect SiO_3^{2-} and SiO_2^0 (Shchapova et al., 2010). The absence of any additional components or variations for Zr3d photo-peak suggests less Zr enrichment or less chemical change occurred on the surface of detrital zircons (Balan et al., 2001). It further supports the better resistance of zircon to weathering and less chances of radiation damage (Balan et al., 2001). The UV-Vis-NIR spectrum of zircon is given in Figure 4(a). It helps to analyze the effect of natural radiation, and thereby the extent of metmictization occurred in zircon. Natural radiation in detrital zircon grain results in the replacement of zirconium with uranium atoms. This can be identified by analyzing with UV-Vis-NIR spectroscopy. The sharp lines of absorption spectra below 600nm in zircon is due to f-f electron transition caused by the presence of U, Th, and rare earth elements (Chen et al., 2011). But in the case of natural zircon, these sharp lines are weak and faint denoting less chances of radiation damage (Nasdala, 2003). The results of Raman, XPS, and UV-Vis-NIR spectroscopy clearly denote less metamictization and a well-crystallized structure for detrital zircon grains.

The rare earth and trace elements present in zircon samples of Varkala and Kovalam are shown in Figure 5 (a1-a2) and Figure 5 (b1-b2). The precision and accuracy of the trace element analysis is less than 2% RSD and 5% RSD for µg/mL and ng/mL-pg/mL levels in the original samples. The total rare-earth content of Varkala and Kovalam zircon are 1574.08ppm and 1823.39ppm with a maximum for Ce, followed by La, Nd, Y, Sc, Pr, etc. The Ce content in Varkala and Kovalam zircon are 605.217ppm and 651.110ppm respecively. The zircon from the Kayamkulam–Thottappally placers, Kerala, southwest India also shows a high concentration of Ce (79.52 – 7615.19ppm) followed by La, Nd, and so on (Nallusamy, 2015). The trace elements present in Varkala and Kovalam account for about 1.781% and 1.753%, in which Zn exists mainly with a concentration of 1.114% and 1.011%, followed by Pb, Hf, Sr, Ba, Th, Cu, etc. The radioactive elements are also present in zircon. The Th content of Varkala and Kovalam zircon are 236.002ppm and 208.843ppm, whereas the U content is 118.049ppm and 151.058ppm. The chondrite–normalised REE

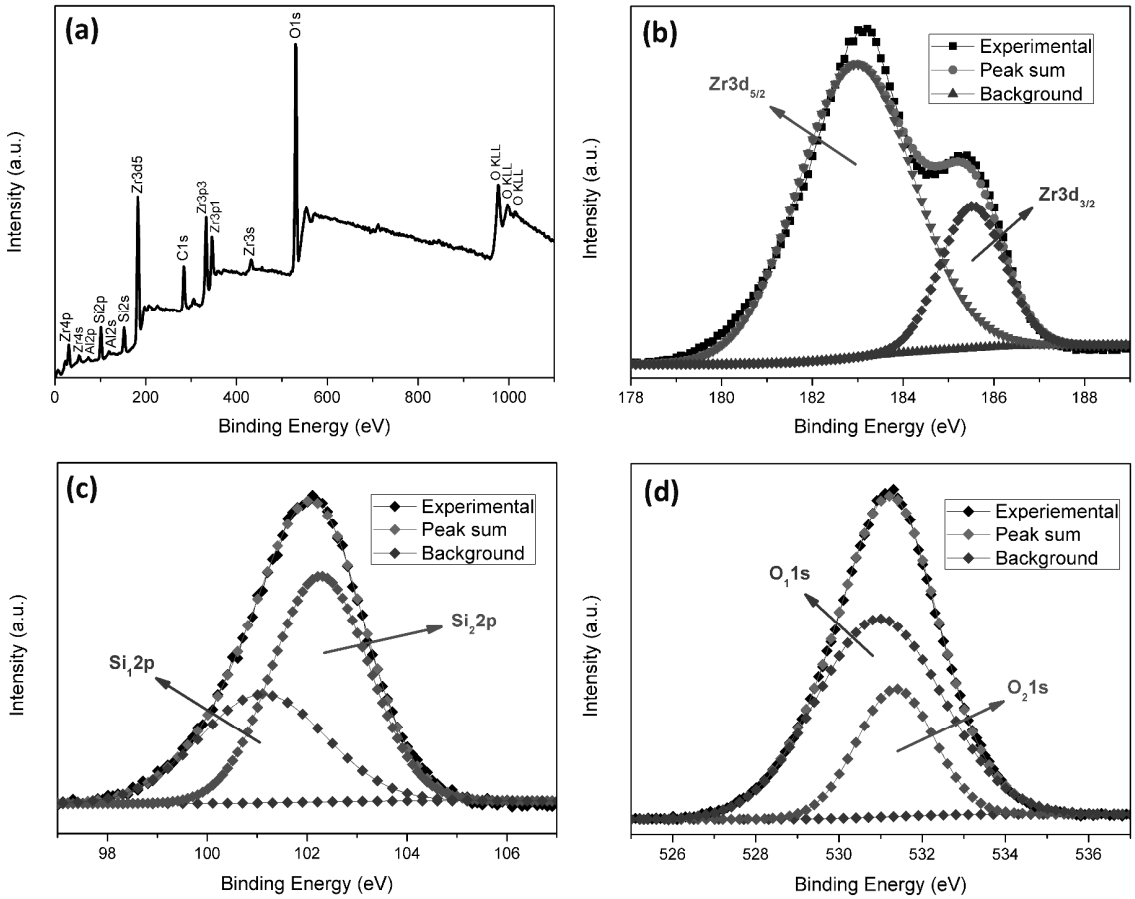

Fig. 3. XPS results of zircon **(a)** Wide scan XPS spectra, and high resolution scans of **(b)** Zr3d, and **(c)** Si2p, and **(d)** O1s.

patterns (Taylor and McLennan, 1985) are given in Fig. 6(a). Like other placer deposits in Kayamkulam, Thottappally, southwest India, the zircons of the present study area also show enrichment for LREE compared to HREE (Nallusamy, 2015). Moreover, a positive Ce-anomaly and a negative Eu-anomaly were also observed (Fig. 6 (a)). This anomalies are characteristic features of unaltered igneous zircon (Hoskin and Schaltegger, 2003). The redox conditions during zircon crystallization from magma make the Eu exist in the state of Eu^{2+} causes negative anomaly for Eu (Murali et al., 1983). The Eu having a larger ionic size, which is against other trivalent rare earth elements, results in its least preference during crystallization, and the preferential uptake of Eu by other phases may cause negative Eu anomaly for detrital zircon (Belousova et al., 2006). The variation in REE concentration reflects the multi-source origin of detrital zircon grains (Hoskin and Ireland, 2000). However, the bulk zircon grains from Varkala and Kovalam have similar REE patterns (Fig.6(a)), which implies the same origin for zircon. Figure 8 shows the SEM micrographs of detrital zircon grains. Zircons are usually stable and well-developed with rounded edges with high relief (Fig.8 (a-f)). The rounded edges suggest a long history of transportation. Presence of more rounded zircon grains in the present study area may be a significant contribution of offshore as suggested by (Mallik, 1986a).

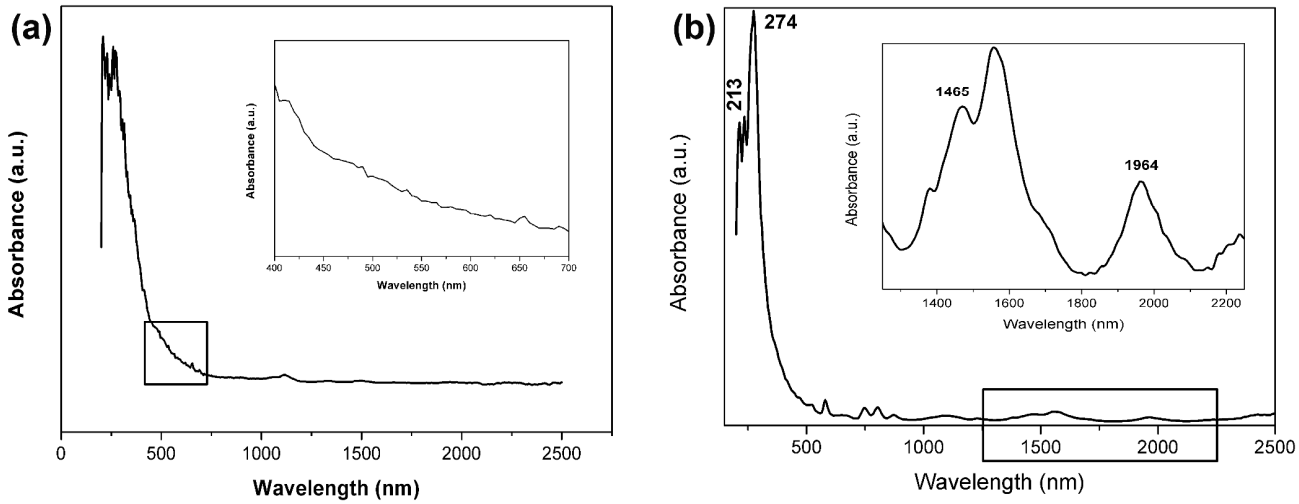

Fig.4. UV-Vis-NIR spectra **(a)** zircon; **(b)** monazite

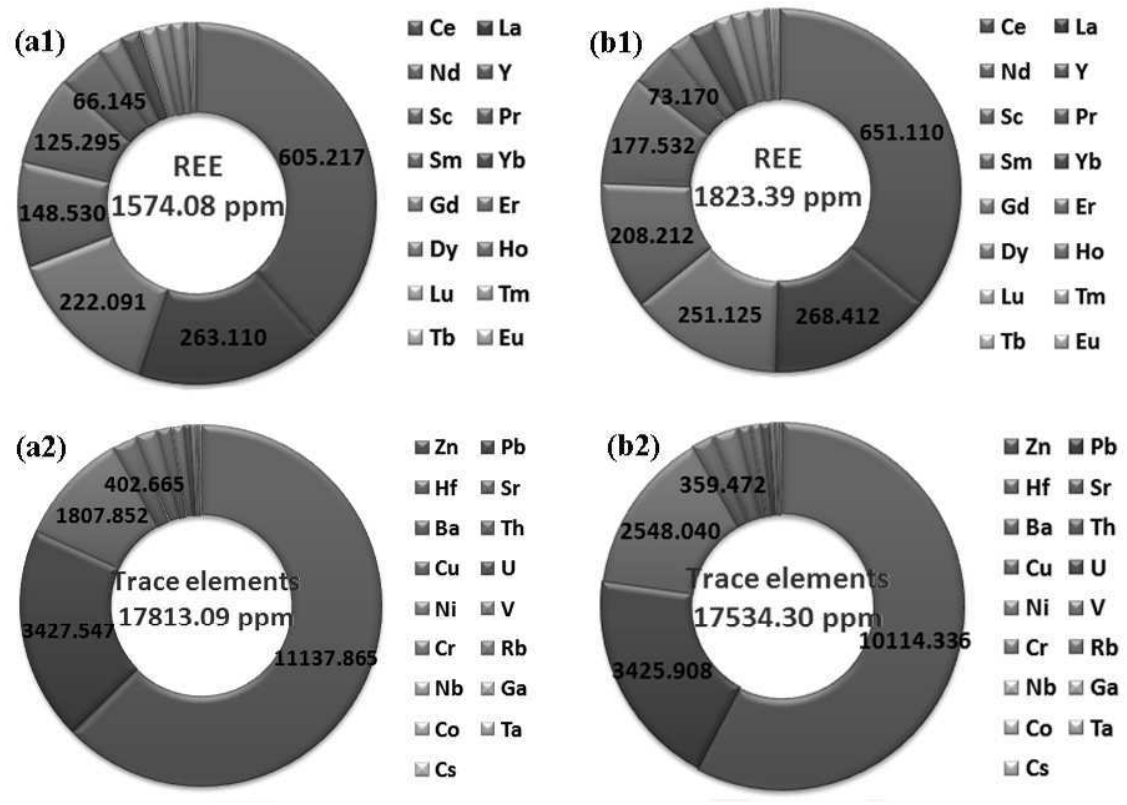

Fig.5. Rare earth elements and trace elements present in zircon. (a1-a2) Varkala; (b1-b2) Kovalam.

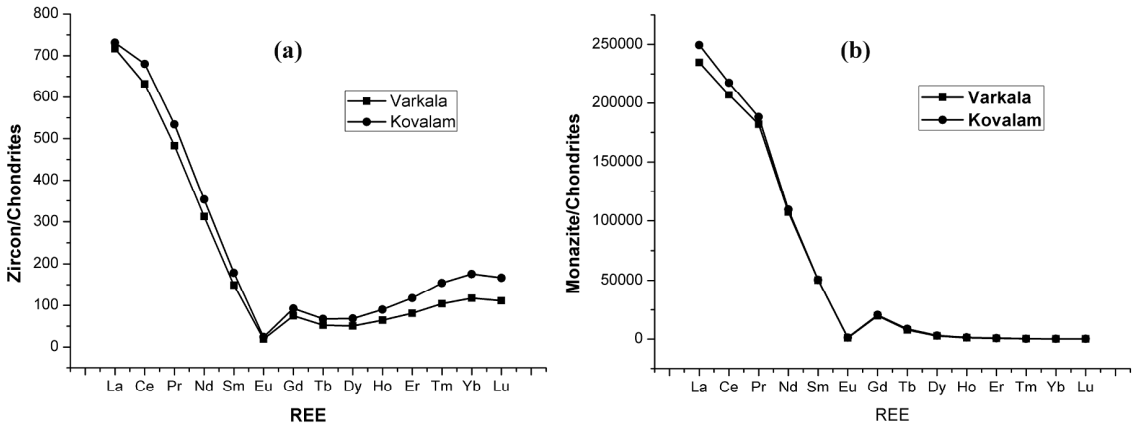

Fig.6. Chondrite–normalised REE patterns **(a)** zircon; **(b)** monazite.

Inclusions, impact V's, and irregular pits of different shapes are seen on the surface. Zoning effects were also noticed on the grains (Mallik, 1986b). These features clearly suggest the derivation of detrital zircons from the charnockite suite of south-west India (Nallusamy, 2015). During transportation, mechanical abrasion may cause the formation of broken grains with many marks and cracks on the surface (Fig. 8 (a, e)). The grain-to-grain collision in the aquatic medium creates V-shaped pits (Roger Higgs (2), 1979). The solution activity causes grooves on the surface-oriented in different angles (Nallusamy, 2015). Even though the khondalite and charnockites of the Western Ghats act as the main source of zircon grains, the incipient charnockite produce a comparatively more number of rounded detrital zircons (Kumar and Narayanaswamy, 1995; Soman, 2002). Figure 9(a) and Table 3 show the SEM-EDS results of the zircon grains. The SEM-EDS of the zircon grains show high content of Zr followed by Si (Routray and Rao, 2011). The Zr and Si content obtained by SEM-EDS is 45.35% and 12.90% (weight percentage), which are also comparable with the zircon from Kayamkulam, Thottappally, southwest India (Nallusamy, 2015). The surface morphological analysis and REE chemistry prove that the detrital zircon of the study area are derived from khondalites and charnockites units, which are commonly seen in the coastal hinterland of the southwest part of Kerala.

Monazite

Monazite is a light rare-earth orthophosphates mineral with the general formula MPO_4 where M = La to Gd. It belongs to the monoclinic system (space group C_{2h}^5) consists of four formula units per unit cell. The M and PO_4 occupy the general *C1* sites. About 36 Raman-active modes (A_g+B_g) are reported for monazite (Ce) as represented by its optical modes as $\tilde{A} = 18A_g + 17A_u + 18B_g + 16B_u$ (Sundararajan et al., 2021). The free $(PO_4)_{3-}$ ion shows the normal

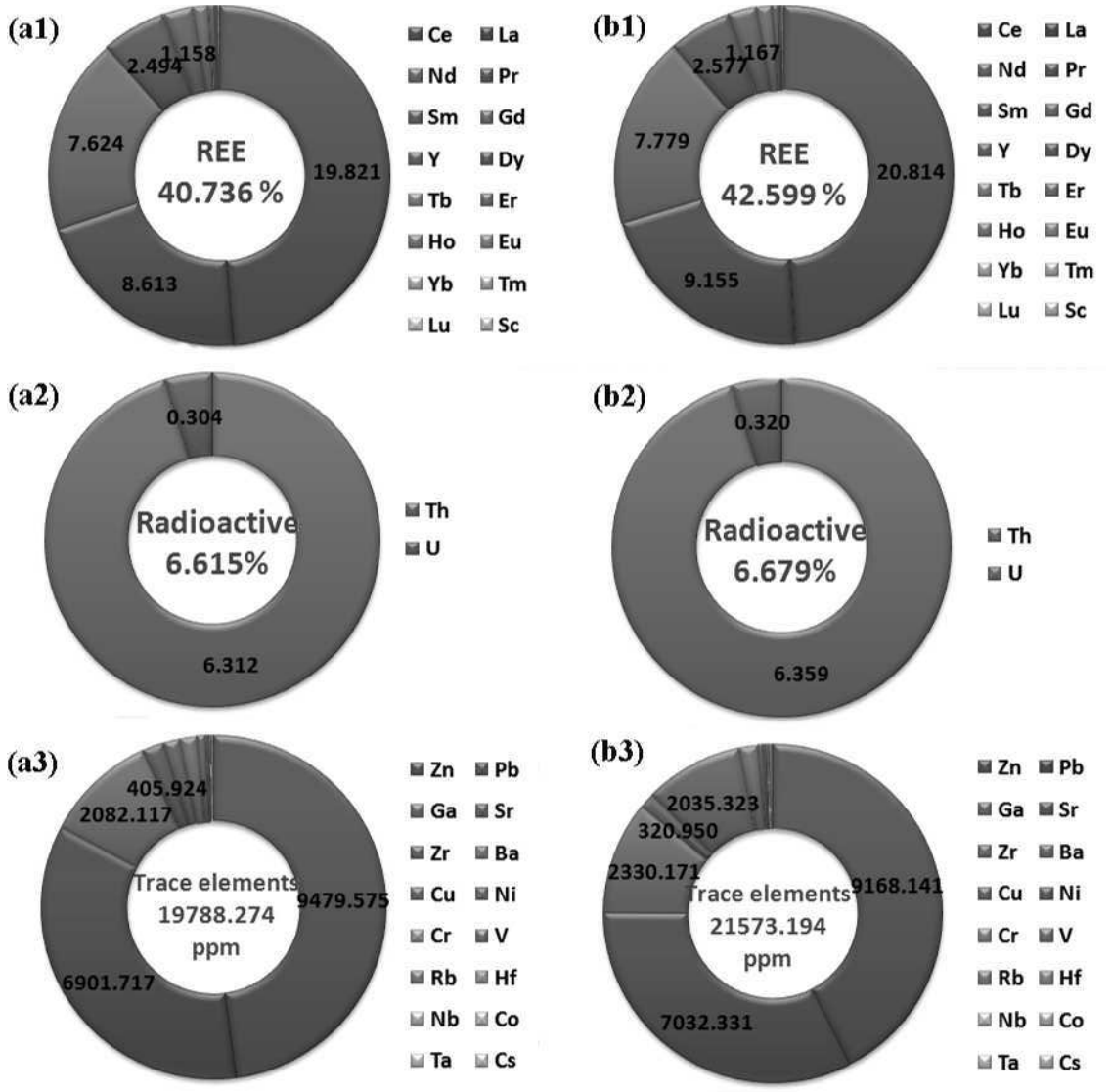

Fig.7. Rare earth elements, radioactive elements and other trace elements present in monazite. (a1-a3) Varkala; (b1-b3) Kovalam.

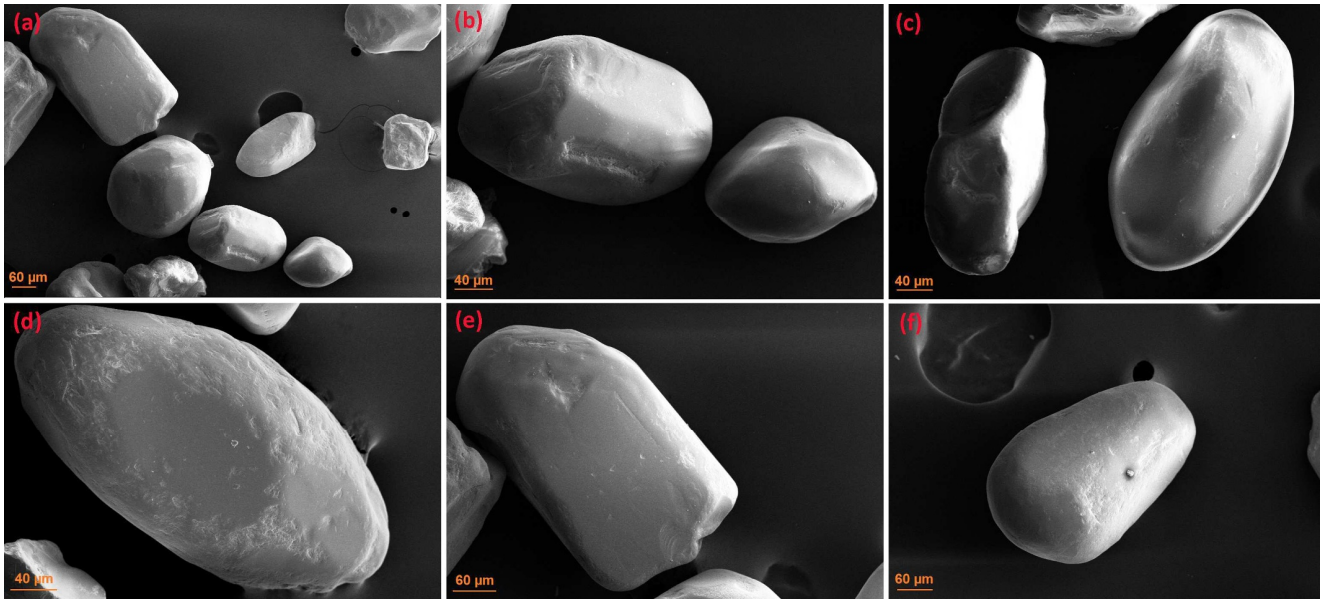

Fig.8. SEM images of zircon

modes, such as v_1, v_3, v_2, and v_4 correspond to symmetric stretch (A1), antisymmetric stretch (F2), bending (E), and (F2) vibrations. The distinct Raman peaks in the range 970- 1075 $cm^{"1}$ correspond to internal PO_4 stretching vibrations (Sadeghi et al., 2020). The Raman modes of monazite were clearly shown in Figure 2(b) and Table 2. The PO_4 bending together with the external vibrations of Ce^{3+} ions and $[PO_4]^{3-}$ units cause peaks below 620 cm^{-1} (Simpraditpan et al., 2013). The strong peak at 972 cm^{-1} corresponds to symmetric stretching of the PO_4 tetrahedrons caused by both A_g and B_g modes. Compared to zircon, monazite doesn't exist in the metamict state, even though it contains a large amount of U and Th (Ewing, 1975). In natural monazite, the radiation damage is limited to isolated areas within the crystal. So radiation damage in monazite is studied by external irradiation or by annealing above the critical temperature where amorphization happens (Meldrum et al., 1998). On annealing the monazite to a temperature of 1200ºC, $v_1(PO_4)$ band shifts from 972 to 974 cm^{-1} with a decrease in FWHM (Seydoux-Guillaume et al., 2002).

The UV-Vis-NIR spectrum of monazite is shown in Figure 4(b). Two absorption bands of 213nm and 274nm in the UV region correspond to the transition of $^2F_{5/2}$ (ground state) to $^2D_{5/2}$ and $^2D_{3/2}$ levels (excited state). The weak extension noticed from 300 to 450nm corresponds to the presence of Ce^{4+}. The peaks around 1465nm and 1964nm in the NIR region corresponds to the presence of phosphate (Verma and Bamzai, 2014). The rare earth elements, radioactive elements, and trace elements present in monazite are shown in Figure 7. The total REE present in monazite from Varkala and Kovalam are 40.736% and 42.599%, with major content of Ce (19.821% and 20.814%) followed by La, Nd, Pr, Sm, Gd, Y, etc. The earlier determined ΣREE using ICP-MS for Chavara and Manavalakurichi monazite is 48.42% and 56.61%, which are comparable to the current results (Rajendran et al., 2008). The Ce content for monazite from Chavara and Manavakurichi is 23.83% and 27.68%, which comes very close to the results of the present study. The Ce present in highest concentration followed by La, Nd, Pr, Sm, and so on. The concentration of radioactive elements such as Th and U present in Varkala are 6.312%

Table 2. Raman active frequencies (cm^{-1}) of Monazite

Symmetry	Assignment	Raman peaks (cm^{-1})
Bg	Lattice	89
Ag	Lattice	105
Ag	Lattice	151
Bg	Lattice	173
Ag	Lattice	181
Ag /Bg	Lattice	219
Ag /Bg	Lattice	227
Ag	Lattice	256
Ag	Lattice	276
Ag/Bg	Lattice	400
Ag/Bg	Lattice	418
Ag/Bg	v_2	469
Ag /Bg	v_4	621
Ag /Bg	v_1	972
Ag /Bg	v_3	1058

Table 3. SEM-EDAX results of zircon

Element	Weight (%)	Atomic (%)
Zr L	45.35	13.94
Si K	12.9	12.88
O K	41.75	73.18

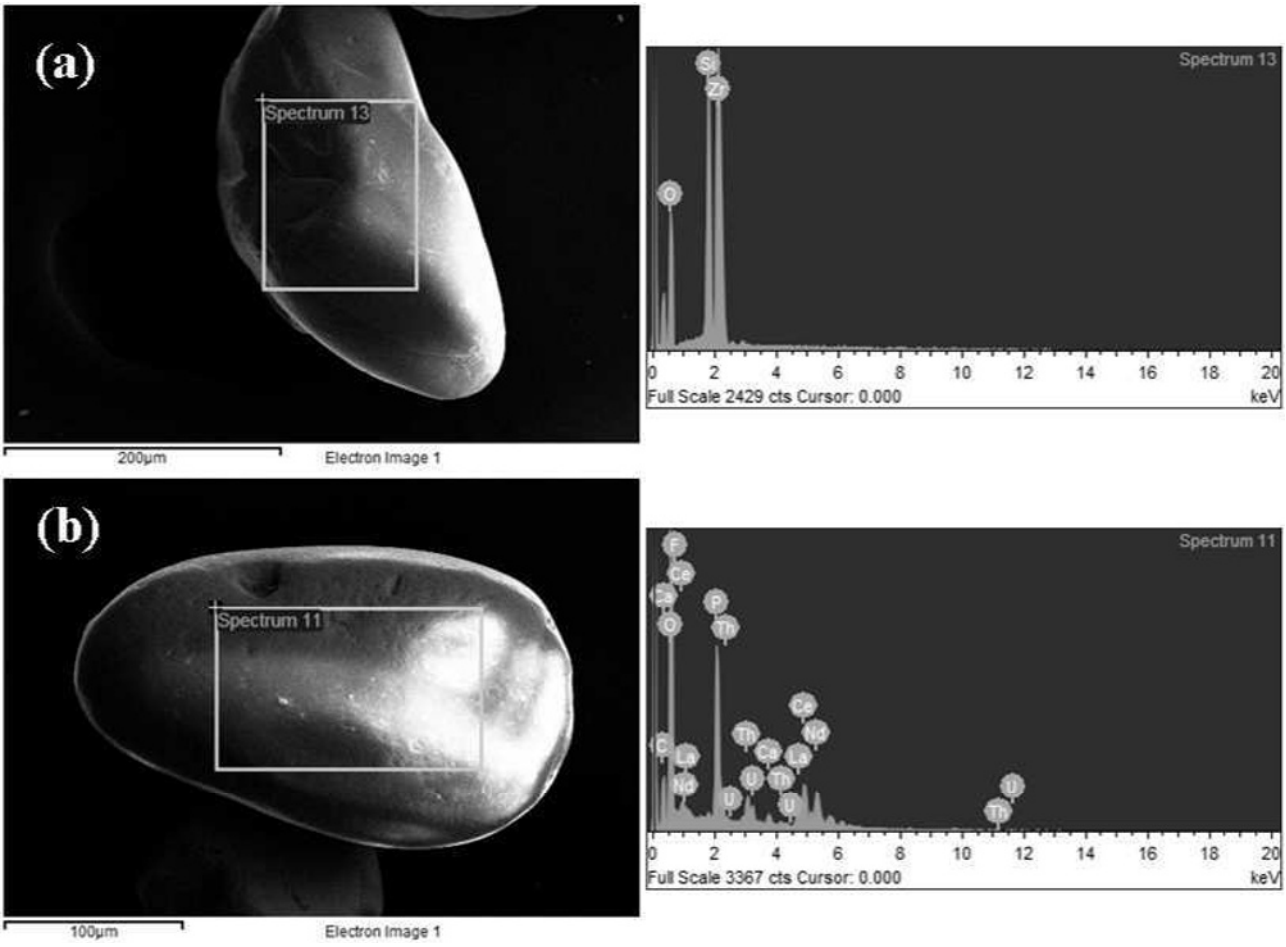

Fig.9. SEM-EDS results. **(a)** zircon; **(b)** monazite.

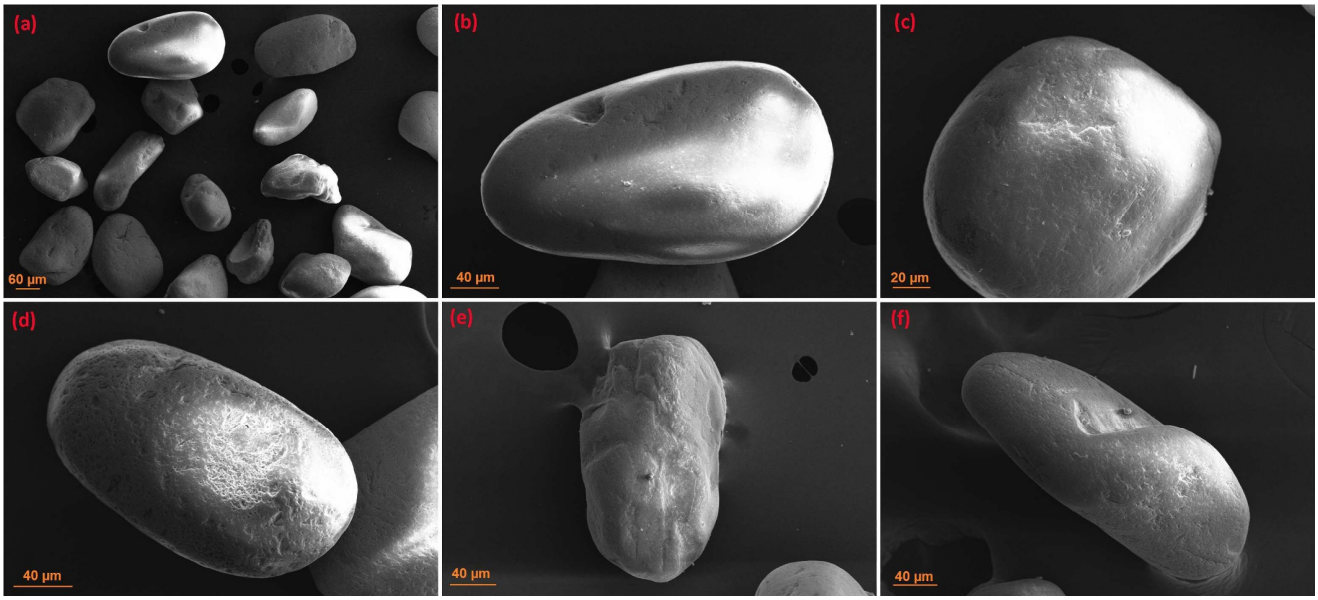

Fig.10. SEM images of monazite.

and 0.304%, and that of Kovalam are 6.359% and 0.320%. The ThO_2 and U_3O_8 content for Chavara and Manavalakurichi monazite normally observed around 10.50% and 0.04%, which are comparable to the current results (Rajendran et al., 2008). The trace element content of Varkala and Kovalam samples is 1.98% and 2.16%, in which the Zn exists majorly, followed by Pb, Ga, Sr, Zr, Ba, etc. The chondrite–normalised REE patterns for bulk monazite grains are drawn by (Taylor and McLennan, 1985) are given in Fig.6(b). It shows a greater enrichment for lighter rare earth elements with a prominent negative Eu anomaly, which is also similar to Chavara and Manavalakurichi detrital monazite (Rajendran et al., 2008). The less variation in REE abundance for both Varkala and Kovalam monazite suggests the existence of the same provenance rocks act as the origin of monazite. The variation in Ce content is 0.993%, which is very less compared to the reported values of Chavara and Manavalakirichi (about 4.45%) (Rajendran et al., 2008).

Figure 10 gives the SEM photos of monazite. Figure 9(b) and Table 4 show the SEM-EDS results of monazite. The monazite is usually seen as highly rounded in shape with moderate relief (Fig.10 (a-d)). Irregular pits oriented in different directions are noticed (Figure 10 (b and d)). Cleavage-controlled blocky fractures due to the removal of blocks (Figure 10 (e and f) were formed due to precipitation. Impact effects cause linear, curved, or irregular features, sometimes they coalesced on the surface (Fig.10 (e)). The morphology clearly indicates the polycyclic nature of the grains occurred due to high physical energy conditions, long transport, and solution effects of grains (Mallik, 1986b). The high content of rare earth elements (Ce, La, and Nd), radioactive elements (Th and U), and P confirms that the minerals are monazite. The Ce content estimated through EDS analysis is 14.31% (weight percentage), whereas that for Chavara monazite is 21.42% (Anitha et al., 2020). The SEM-EDS also shows the minor presence of Ca and F (Anitha et al., 2020).

Table 4. SEM-EDAX results of monazite

Element	Weight (%)	Atomic (%)
Ce L	14.31	2.3
La L	6.99	1.13
Nd L	4.8	0.75
Th M	5.81	0.56
U M	0.15	0.01
P K	9.84	7.14
Ca K	0.8	0.45
F K	0.09	0.11
O K	41.89	58.87
C K	15.31	28.67

CONCLUSION

Detailed studies on the crystal structure, REE chemistry, and surface morphology of detrital zircon and monazite grains collected from the coasts of Varkala and Kovalam, southwest of India, were carried out using Raman spectroscopy, XPS, UV-Vis-NIR spectroscopy, HR-ICP-MS, and SEM-EDS analysis. The Raman-XPS peaks confirm less metamictization for zircon and monazite samples. The REE chemistry and surface morphological studies provide information regarding the provenance of detrital zircon and monazite. Further, the SEM images show the mechanical impacts and solution pits, a clear indication of weathering and long transportation process.

Acknowledgement: R. G. Rejith is thankful to the DST-INSPIRE Division, Department of Science & Technology (DST), Government of India for providing the INSPIRE fellowship. The authors thank the Director, CSIR-National Institute for Interdisciplinary Science and Technology (CSIR-NIIST), Thiruvananthapuram, Kerala, India for extending the laboratory facilities.

References

Ali, M.A., Krishnan, S., Banerjee, D.C. (2001) Beach and inland heavy mineral sand investigations and deposits in india-An overview. Explor. Res. At. Miner., v.13, pp.1–21.

Angusamy, N., Dajkumar Sahayam, J., Suresh Gandhi, M., Rajamanickam, G.V. (2005) Coastal Placer Deposits of Central Tamil Nadu, India. Mar. Georesources Geotechnol., v.23, pp.137–174. doi:10.1080/10641190500192102

Angusamy, N., Loveson, V.J., Rajamanickam, G.V. (2004) Zircon and ilmenite from the beach placers of southern coast of Tamil Nadu, east coast of India. Indian Jour. Mar. Sci., v.33, pp.138–149.

Anitha, J.K., Joseph, S., Rejith, R.G., Sundararajan, M. (2020) Monazite chemistry and its distribution along the coast of Neendakara–Kayamkulam belt, Kerala, India. SN Appl. Sci., v.2, pp.812. doi:10.1007/s42452-020-2594-6

Balan., Trocellier, P., Jupille, J., Fritsch, E., Muller, J., Calas, G., (2001) Surface chemistry of weathered zircons. Chem. Geol., v.181, pp.13–22. doi:10.1016/S0009-2541(01)00271-6

Balan, E., Neuville, D.R., Trocellier, P., Fritsch, E., Muller, J.P., Calas, G. (2001) Metamictization and chemical durability of detrital zircon. Am.

Mineral., v.86, pp.1025–1033. doi:10.2138/am-2001-8-909
Balaram, V. (2019) Rare earth elements: A review of applications, occurrence, exploration, analysis, recycling, and environmental impact. Geosci. Front. doi:10.1016/j.gsf.2018.12.005
Banerjee, G. (1998) Beach and minerals: A new material resource for glass and ceramics. Bull. Mater. Sci., v.21, pp.349–354. doi:10.1007/BF02744965
Bangaku Naidu, K., Reddy, K.S.N., Sekhar, C.R., Ganapati Rao, P., Murali Krishna, K.N. (2016) REE geochemistry of monazites from coastal sands between Bhimunipatnam and Konada, Andhra Pradesh, East coast of India. Curr. Sci., v.110, pp.1550-1159. doi:10.18520/cs/v110/i8/1550-1559
Belousova, E.A., Griffin, W.L., O'Reilly, S.Y. (2006) Zircon crystal morphology, trace element signatures and Hf isotope composition as a tool for oetrogenetic modelling: Examples from Eastern Australian granitoids. Jour. Petrol. doi:10.1093/petrology/egi077
Chandrasekar, N., Mujabar, P.S., Rajamanickam, G.V. (2011) Investigation of heavy-mineral deposits using multispectral satellite data. Int. Jour. Remote Sens., v.32, pp.8641–8655. doi:10.1080/01431161.2010.545448
Chen, T., Ai, H., Yang, M., Zheng, S., Liu, Y. (2011) Brownish red zircon from Muling, China. Gems Gemol. doi:10.5741/GEMS.47.1.36
Dawson, P., Hargreave, M.M., Wilkinson, G.R. (1971) The vibrational spectrum of zircon (zrsio 4). Jour. Phys.: C Solid State Phys., v.4, pp.240–256. https://doi.org/10.1088/0022-3719/4/2/014
Ewing, R.C. (1994) The metamict state: 1993 — the centennial. Nucl. Instruments Methods Phys. Res. Sect. B Beam Interact. with Mater. Atoms., v.91, pp.22–29. doi:10.1016/0168-583X(94)96186-7
Ewing, R.C. (1975) The crystal chemistry of complex niobium and tantalum oxides. IV. The metamict state: Discussion | American Mineralogist | GeoScienceWorld. Am. Mineral., v.60, pp.728–733.
Ferron, C.J., Bulatovic, S.M., Salter, R.S. (1991) Beneficiation of Rare Earth Oxide Minerals. Mater. Sci. Forum. doi:10.4028/www.scientific.net/msf.70-72.251
Gayathri, G.S., Rejith, R.G., Jeelani, S.H., Sundararajan, M., Aslam, M.M., Chidambaram, S. (2017) Heavy Mineral Resources In Tamil Nadu, India: An Overview. *In:* Geochemistry and Mineralogy of Coastal Sediments in Tamil Nadu. pp.110–121.
Gayathri, G.S., Sundararajan, M., Rejith, R.G., Sreela, S.R., Silambarasan, S., Pruthiviraj, N. (2021) Texture and mineralogy of beach sediments of Chavara and Manavalakurichi, South India-A comparative analysis. Indian Jour. Geol. Mar. Sci., v.50, pp.203–211.
Hazen, R.M., Finger, L.M. (1979) Crystal structure and compressibility of zircon at high pressure. Am. Mineral., v.64, pp.196–201.
Holland, H.D., Gottfried, D. (1955) The effect of nuclear radiation on the structure of zircon. Acta Crystallogr., v.8, pp.291–300. doi:10.1107/S0365110X55000947
Hoskin, P.W.O., Ireland, T.R. (2000) Rare earth element chemistry of zircon and its use as a provenance indicator. Geology. doi:10.1130/0091-7613(2000)028<0627:REECOZ>2.3.CO;2
Hoskin, P.W.O., Rodgers, K.A. (1996) Raman spectral shift in the isomorphous series (Zr1-xHfx)SiO_4. Eur. Jour. Solid State Inorg. Chem., v.33, pp.1111-1121.
Hoskin, P.W.O., Schaltegger, U. (2003) The composition of zircon and igneous and metamorphic petrogenesis. Rev. Mineral. Geochemistry. doi:10.2113/0530027
Krishnan, S., Viswanathan, G., Balachandran, K. (2001) Heavy mineral sand deposits of kerala. Explor. Res. At. Miner., v.13, pp.111–146.
Kumar, G.R.R., Narayanaswamy, (1995) Morphology of zircons in massive and incipient charnockites of southern Kerala: Their bearing on the origin. Curr. Sci., v.69, pp.941–944. doi:10.2307/24097217
Kumari, A., Panda, R., Jha, M.K., Kumar, J.R., Lee, J.Y. (2015) Process development to recover rare earth metals from monazite mineral: A review. Miner. Eng., v.79, pp.102–115. doi:10.1016/j.mineng.2015.05.003
Lomenech, C., Simoni, E., Drot, R., Ehrhardt, J.-J., Mielczarski, J. (2003) Sorption of uranium (VI) species on zircon: structural investigation of the solid/solution interface. Jour. Colloid Interface Sci., v.261, pp.221–232. doi:10.1016/S0021-9797(03)00101-2
Lumpkin, G.R. (2001) Alpha-decay damage and aqueous durability of actinide host phases in natural systems. Jour. Nucl. Mater., v.289, pp.136–166. doi:10.1016/S0022-3115(00)00693-0
Mallik, T.K. (1986a) Micromorphology of some placer minerals from Kerala beach, India. Mar. Geol., v.71, pp.371–381. doi:10.1016/0025-3227(86)90079-4
Mallik, T.K. (1986b) Micromorphology of some placer minerals from Kerala beach, India. Mar. Geol., v.71, pp.371–381. doi:10.1016/0025-3227(86)90079-4
Meldrum, A., Boatner, L.A., Weber, W.J., Ewing, R.C. (1998) Radiation damage in zircon and monazite. Geochim. Cosmochim. Acta. doi:10.1016/S0016-7037(98)00174-4
Mitchell, C.J., Yusof, M.A. (1993) Beneficiation and appraisal of a beach placer sand deposit from Malawi. Rare Earth Miner. Chem. Orig. Ore Depos. London, UK.
Mohanty, A.K., Das, S.K., Vijayan, V., Sengupta, D., Saha, S.K., (2003) Geochemical studies of monazite sands of Chhatrapur beach placer deposit of Orissa, India by PIXE and EDXRF method. Nucl. Instruments Methods Phys. Res. Sect. B Beam Interact. with Mater. Atoms. doi:10.1016/S0168-583X(03)01166-2
Moustafa, M.I., Abdelfattah, N.A. (2010) Physical and chemical beneficiation of the egyptian beach monazite. Resour. Geol. doi:10.1111/j.1751-3928.2010.00131.x
Murali, A.V., Parthasarathy, R., Mahadevan, T.M., Das, M.S., (1983) Trace element characteristics, REE patterns and partition coefficients of zircons from different geological environments-A case study on Indian zircons. Geochim. Cosmochim. Acta. doi:10.1016/0016-7037(83)90220-X
Nageswara Rao, M., Dikshitulu, G.R., Desapati, T., Krishnan, S., Mir Azam Ali (2001) A strategic placer mineral deposit along Tandava-Varaha rver coastal area, Visakhapatnam district, Andhra Pradesh. JOAMS 7.
Naher, S., Haseeb, A.S.M.A. (2006) A technical note on the production of zirconia and zircon brick from locally available zircon in Bangladesh. Jour. Mater. Process. Technol. doi:10.1016/j.jmatprotec.2005.10.013
Nallusamy, B. (2015) Morphology, Trace, and Rare Earth Elements of Detrital Zircon of Kayamkulam, Thottappally Placers, South West India—Implications for Provenance. Mar. Georesources Geotechnol. doi:10.1080/1064119X.2014.952855
Nasdala, L. (2003) Spectroscopic methods applied to zircon. Rev. Mineral. Geochemistry, v.53, pp.427–467. doi:10.2113/0530427
Nasdala, L., Irmer, G., Wolf, D. (1995) The degree of metamictization in zircon: a Raman spectroscopic study. Eur. Jour. Mineral., 7, 471–478. doi:10.1127/ejm/7/3/0471
Rabie, K.A. (2007) A group separation and purification of Sm, Eu and Gd from Egyptian beach monazite mineral using solvent extraction. Hydrometallurgy. doi:10.1016/j.hydromet.2005.12.012
Rajan Girija, R., Mayappan, S. (2019) Mapping of mineral resources and lithological units: a review of remote sensing techniques. Int. Jour. Image Data Fusion. doi:/10.1080/19479832.2019.1589585
Rajendran, J., Balasubramanian, G., Thampi, P.K. (2008) Determination of rare earth elements in Indian coastal monazite by ICP-AES and ICP-MS analysis and their geochemical significance. Curr. Sci., v.94, pp.1296–1302.
Raju, R.D., Ravi, G.S., Shivkumar, K., Reddy, L.S.R., Rohatgi, S. (2005) WDXRFS method for quantification of heavy minerals in sand samples. Jour. Geol. Soc. India, v. 66, pp.401.
Rejith, R.G., Sundararajan, M. (2018) Combined magnetic, electrostatic, and gravity separation techniques for recovering strategic heavy minerals from beach sands. Mar. Georesources Geotechnol., v.36, pp.959–965. doi:10.1080/1064119X.2017.1403523
Rejith, R.G., Sundararajan, M., Gnanappazham, L., Loveson, V.J., (2020a) Satellite-based spectral mapping (ASTER and landsat data) of mineralogical signatures of beach sediments: a precursor insight. Geocarto Int., pp.1–24. doi:10.1080/10106049.2020.1750061
Rejith, R.G., Sundararajan, M., Peer Mohamed, A., Satyanarayanan, M. (2021) Raman-XPS spectroscopy, REE chemistry, and surface morphology of Fe-Ti oxide heavy mineral sands: a case study from Varkala-Kovalam coast, south-west India. Appl. Earth Sci., pp.1–13. doi:10.1080/25726838.2021.1911584
Rejith, R.G., Sundararajan, M., Mohammed-Aslam, M.A., (2020b) Remote sensing for exploring heavy mineral deposits: a case study of Chavara and Manavalakurichi deposits, southwest coast of India, *In:* Remote Sensing of Ocean and Coastal Environments 1st Edition. Elsevier, pp.177–188.
Renjith, R.A., Rejith, R.G., Sundararajan, M. (2020) Evaluation of coastal sediments: an appraisal of geochemistry using ED-XRF and GIS techniques, in: Remote Sensing of Ocean and Coastal Environments 1st

Edition. Elsevier, pp.99–116.

Roger Higgs (2), (1979) Quartz-Grain Surface Features of Mesozoic-Cenozoic Sands from the Labrador and Western Greenland Continental Margins. SEPM Jour. Sediment. Res., v.49. doi:10.1306/212F779D-2B24-11D7-8648000102C1865D

Routray, S., Rao, R.B. (2011) Beneficiation and Characterization of Detrital Zircons from Beach Sand and Red Sediments in India. Jour. Miner. Mater. Charact. Eng., v.10, pp.1409–1428. doi:10.4236/jmmce.2011.1015110

Sadeghi, K., Thanakkasaranee, S., Lim, I.-J., Seo, J. (2020) Calcined marine coral powders as a novel ecofriendly antimicrobial agent. Mater. Sci. Eng., C 107, 110193. doi:10.1016/j.msec.2019.110193

Sajimol, S., Rejith, R.G., Lakshumanan, C., Sundararajan, M., 2017. Sedimentology And Geochemistry Of Heavy Mineral Deposits along the Coast of Kanyakumari District, Tamil Nadu, India, *In:* Geochemistry and Mineralogy of Coastal Sediments in Tamil Nadu. pp.145–161.

Samsonov, M.D., Trofimov, T.I., Kulyako, Y.M., Vinokurov, S.E., Malikov, D.A., Batorshin, G.S., Myasoedov, B.F. (2015) Recovery of rare earth elements, uranium, and thorium from monazite concentrate by supercritical fluid extraction. Radiochemistry. doi:10.1134/S1066362215040025

Sathasivam, S., Kankara, R.S., Selvan, S.C., Muthusamy, M., Samykannu, A., Bhoopathi, R. (2015) Textural Characterization of Coastal Sediments along Tamil Nadu Coast, East Coast of India. Procedia Eng., v.116, pp.794–801. doi:10.1016/j.proeng.2015.08.366

Satyanarayanan, M., Balaram, V., Sawant, S.S., Subramanyam, K.S.V., Krishna, G.V., Dasaram, B., Manikyamba, C. (2018) Rapid determination of REEs, PGEs, and other trace elements in geological and environmental materials by high resolution inductively coupled plasma mass spectrometry. At. Spectrosc., v.39, pp.1–15.

Seydoux-Guillaume, A.M., Wirth, R., Nasdala, L., Gottschalk, M., Montel, J.M., Heinrich, W. (2002) An XRD, TEM and Raman study of experimentally annealed natural monazite. Phys. Chem. Miner. doi:10.1007/s00269-001-0232-4

Shchapova, Y. V., Votyakov, S.L., Kuznetsov, M. V., Ivanovskii, A.L.(2010) Effect of Radiation Defects on the Electronic Structure of Zircon by X-Ray Photoelectron Spectroscopy Data. Jour. Struct. Chem., v.51, pp.657–662. doi:10.1007/s10947-010-0096-x

Simpraditpan, A., Wirunmongkol, T., Pavasupree, S., Pecharapa, W. (2013) Hydrothermal Synthesis of Nanofibers from Natural Ilmenite Mineral and Their Utilization for Dye-Sensitized Solar Cell. Integr. Ferroelectr. v.149, pp.135–142. doi:10.1080/10584587.2013.853592

Soman, K. (2002) Geology of Kerala. Geological Society of India, Bangalore, 336p.

Sundararajan, M. (2018) Occurrence, Distribution and grain micro-textures of light heavy placer minerals in thiruchendur-ovari beaches, South-Eastern coast of India. v.20, pp.399–411.

Sundararajan, M., Bhat, K.H., Babu, N., Janaki, M.E.K., Das, P.N.M. (2009) Characterization Studies on Ilmenite of Ullal and Suratkal along Karnataka Coastline, West Coast of India. Jour. Miner. Mater. Charact. Eng., v.08, pp.479–493. doi:10.4236/jmmce.2009.86042

Sundararajan, M., Bhat, K.H., Velusamy, S. (2010) Investigation on mineralogical and chemical characterization of ilmenite deposits of Northern Kerala Coast, India. Res. Jour. Earth Sci., v.2, pp.36–40.

Sundararajan, M., Rejith, R.G., Renjith, R.A., Mohamed, A.P., Gayathri, G.S., Resmi, A.N., Jinesh, K.B., Loveson, V.J. (2021) Raman-XPS spectroscopic investigation of heavy mineral sands along Indian coast. Geo-Marine Lett., v.41. doi:10.1007/s00367-021-00694-8

Syme, R.W.G., Lockwood, D.J., Kerr, H.J. (1977) Raman spectrum of synthetic zircon ($ZrSiO_4$) and thorite ($ThSiO_4$). Jour. Phys. C Solid State Phys., doi:10.1088/0022-3719/10/8/036

Taylor, Y., McLennan, S.M. (1985) The continental crust: Its composition and evolution. Blackwell, Oxford.

Tirumalesh, K., Chidambaram, S. Pethaperumal, S. Sundararajan, M., Thilagavathi, R., Thivya, C., Sharma, D.A., Sinha, U.K. (2020) Geochemical and ^{13}C trends in sedimentary deposits of coastal Pondicherry region, East coast of India – Insights from a borehole study. Geochemistry, v.80, 125553.

Verma, S., Bamzai, K.K. (2014) Preparation of Cerium Orthophosphate Nanosphere by Coprecipitation Route and Its Structural, Thermal, Optical, and Electrical Characterization. Jour. Nanoparticles, pp.1–12. doi:10.1155/2014/125360

Viveganandan, S., Lakshumanan, C., Sundararajan, M., Eswaramoorthi, S., Natesan, U. (2013) Depositional environment of sediments along the Cuddalore coast of Tamilnadu, India. Indian Jour. Mar. Sci., v.42, pp.375–382.

Weber, W.J., Ewing, R.C., Angell, C.A., Arnold, G.W., Cormack, A.N., Delaye, J.M., Griscom, D.L., Hobbs, L.W., Navrotsky, A., Price, D.L., Stoneham, A.M., Weinberg, M.C. (1997) Radiation Effects in Glasses Used for Immobilization of High-level Waste and Plutonium Disposition. Jour. Mater. Res., v.12, pp.1948–1978. doi:10.1557/JMR.1997.0266

Yamagata, C., Andrade, J.B., Ussui, V., Lima, N.B., Paschoal, J.O.A. (2008) High purity zirconia and silica powders via wet process: Alkali fusion of zircon sand, *in:* Materials Science Forum.

Zhang, M., Salje, E.K.H., Farnan, I., Graeme-Barber, A., Daniel, P., Ewing, R.C., Clark, A.M., Leroux, H. (2000) Metamictization of zircon: Raman spectroscopic study. Jour. Phys. Condens. Matter, v.12, pp.1915–1925. doi:10.1088/0953-8984/12/8/333